Hebbian learning in the agglomeration of conducting particles

M. Sperl, A. Chang, N. Weber, and A. Hübler
Center for Complex Systems Research, Department of Physics, Beckman Institute, University of Illinois at Urbana–Champaign, Urbana, Illinois 61801
(Received 2 July 1998)

The Hebbian learning rule is a fundamental concept in the learning of a neuronal net, where a frequently used connection of two neurons is continually reinforced. We study the properties of self-assembling connections of conducting particles in a dielectric liquid, and find that the strength of the connection between different electrodes represents a memory for the history of the system. Optimal parameters and sequences of stimulation for effective training are determined. We discuss a future application of our results for the implementation of a nonvolatile neuronal network based on self-assembling nanowires on a semiconductor surface.
[S1063-651X(99)03603-X]

PACS number(s): 81.10.Dn, 45.05.+x, 05.70.Ln, 84.32.−y

Hebb describes the strengthening of neuronal connections as a mechanism for learning in the human brain [1–3]. The more a connection between neurons in the dendritic structure of axons is used, the stronger is this connection in the future. This process is known as Hebbian learning and is frequently used in neuronal networks.

Dendritic structures are well studied in crystal growth [4] and can be explained in the relatively simple model of diffusion-limited aggregation (DLA) wherein a random walk models the Brownian motion of the particles that aggregate to clusters [5–7]. In a system of self-assembling metallic particles in an electric field the dynamics is governed by electromagnetic interactions and yields self-organizing fractal patterns when a large flux of electric current and a high frictional force are present [8]. The fractal dimension of the emerging patterns was determined for different geometries of the electrodes [9–11]. In contrast to DLA-grown structures, these dendritic patterns self-repair after small perturbations. This property leads to the hypothesis of the principle of minimum resistance in dendritic patterns [9].

In experiments with a pair of electrodes across which a voltage is applied, steel spheres initially dispersed in the vicinity of these electrodes are drawn together by the electric field to form connected, conductive wires. It has been proven analytically that this agglomeration process minimizes the resistance of such a system [12]. Therefore, these wires are stable.

In our experiment (Fig. 1) three point-electrodes are used to induce time-dependent boundary conditions upon the cylindrical cell. A voltage is applied between only two electrodes at any given time. Although the electric field, which drives the wire formation exists for only one electrode pair at a time, after alternating several times the pair to which the voltage is applied, it is found that separate wires can exist for each pair. The electric field that constructs a wire between one pair simultaneously acts to destroy or pull in the wire of the other pair. We find that a wire consists of more particles if the corresponding electrodes induce an electric field more often or for a longer period of time.

The strength of a connection, i.e., the number of particles between the electrodes, depends on the usage and thus represents a memory of the history of the system in the sense of Hebbian learning.

In the experiment (Fig. 1) N spherical steel particles (radius $\rho=1.0$ mm, mass $m=33.0$ mg) are distributed randomly in a cylindrical cell at a constant concentration of particles per area, $C_p=2.5/\mathrm{cm}^2$. The cell is filled with castor oil (viscosity: $\eta=5.68$ Pa s) to a height $h=3$ mm. The oil has a high dielectric constant $\epsilon_{\mathrm{oil}}\approx 4.7$ and a small electrical conductivity $\sigma_{\mathrm{oil}}\leqslant 10^{-12}$ $(\Omega\mathrm{m})^{-1}$. The tips of the electrodes S, A, and B touch the bottom of the cell and form the angle $\theta=\angle ASB$. A and B lie at a radial distance of $d=3$ cm on a circle centered at electrode S.

At the start of the experiment, the particles are at rest and distributed randomly. A voltage of 19.5 kV is applied between the electrodes S and A for time T_A. Thereafter, the voltage is switched to S and B for T_B. This procedure is repeated five times as shown in Fig. 2. A typical initial distribution of the particles is shown in Fig. 3(a).

The dynamics of a single particle at r_i in the electric field is described [12] by a force,

$$\vec{F}_i=-\sum_{j\neq i}\frac{\epsilon_{\mathrm{oil}}}{2\sigma_{\mathrm{oil}}}I_{ij}^2\nabla_{r_{ij}}R_{ij}=6\pi\eta\rho\dot{r}_i, \tag{1}$$

dependent on the currents I_{ij} and resistances R_{ij} between the particles at r_i and r_j. Inertial forces are small compared to the friction and are therefore neglected. The total resistance can then be written as a Lyapunov function, and the resulting dynamics minimizes the total resistance of the system [12] in reaching a stationary state. The resistance drops to zero if a

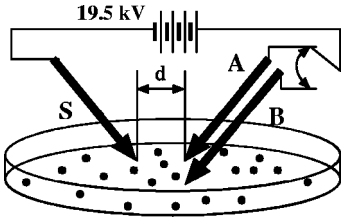

FIG. 1. Experimental setup. Spherical steel particles are distributed randomly at a density $C_p=2.5/\mathrm{cm}^2$ in a cylindrical cell filled with castor oil. The voltage of 19.5 kV is applied to S. A and B are connected alternately.

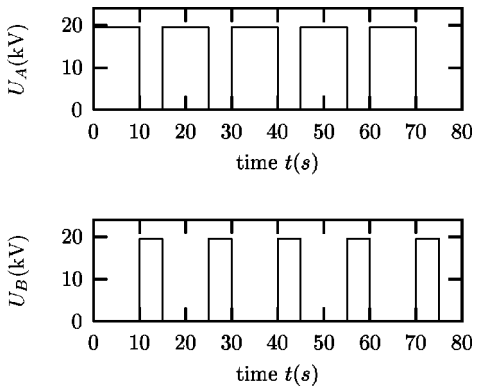

FIG. 2. Applied voltage as a function of time. The voltage of $U_A=19.5$ kV is applied to connection A-S for T_A (here $T_A=10$ s). Subsequently, electrode A is disconnected and the voltage is applied to electrode B ($U_B=19.5$ kV) for $T_B=5$ s. The voltage is switched from A to B and vice versa five times. This sequence constitutes ten changes in boundary conditions, numbered 1 through 10.

complete wire forms. The average time for the formation of a complete wire is $T_c\approx 200$ s at an electrode separation distance $d=3$ cm.

In our experiment such a stationary state is not reached because the boundary conditions are modified before a wire is completed (Fig. 2). The time interval before switching the current to the other electrode never exceeds 0.25 T_c.

The number of particles N_A and N_B between S and the electrodes A or B are determined as indicated in Fig. 3(b). All particles along the A-S axis with centers inside the plotted arcs, which enclose this axis, are counted for N_A, similarly for N_B. These two curved regions have a maximum width of 4 mm at their centers.

The connection between one pair of electrodes is considered to be stronger than the connection between the other pair if the number of particles in the described area is larger in the former than in the latter. In Fig. 3(b), $N_A>N_B$. The connection A-S is stronger than B-S, although voltage was last applied to the connection B-S.

For further discussion, N_A and N_B are normalized in Eq. (2) and Eq. (3) to yield w_{AS} and w_{BS}, the relative strengths of the connections

$$w_{AS}=\frac{N_A}{N_A+N_B}, \tag{2}$$

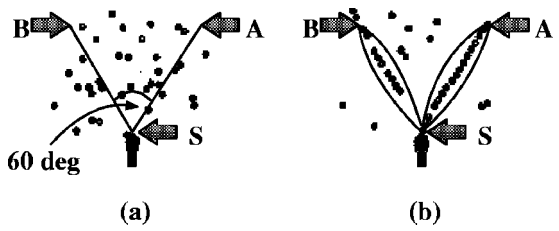

FIG. 3. Initially the particles are distributed randomly, (a). The positions of the electrodes S, A, and B are indicated by the arrows. Axis A-S and axis B-S form the angle θ (here $\theta=60°$). Picture (b) shows the distribution of the particles after step 8 and the area used to determine the number of particles for each connection. Although step 8 used connection B-S, there are still more particles on the axis A-S: $N_A=14$, $N_B=10$, $d=3$ cm, $\theta=60°$, $C_p=2.5/\text{cm}^2$, $r=0.67$.

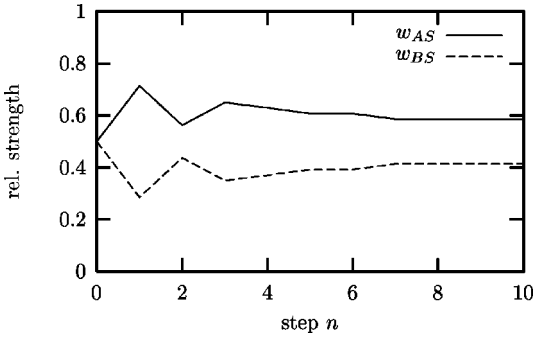

FIG. 4. Relative strengths w_{AS} and w_{BS} after each step at $d=3$ cm, $\theta=60°$, $C_p=2.5/\text{cm}^2$, $r=0.67$. The typical dynamics of the relative strength of connections A-S and B-S exhibits a stationary state after a few steps.

$$w_{BS}=\frac{N_B}{N_A+N_B}. \tag{3}$$

A typical evolution of these strengths is plotted in Fig. 4. A stationary state is achieved after several steps.

The periods for the application of the voltage are also normalized, yielding the stimulation ratio $r=T_A/(T_A+T_B)$. T_A is varied, whereas $T_B=5$ s remains the same.

w_{AS} is measured for different ratios r and angles θ. To quantify the stability of the connections, we take the average over the last two steps of each series and define the average strength $\overline{w}_{AS}$ of the connection A-S after 10 steps in Eq. (4).

$$\overline{w}_{AS}=\frac{w_{AS}(n=9)+w_{AS}(n=10)}{2}. \tag{4}$$

The results show (see Fig. 5) that the mean value for $\overline{w}_{AS}$ increases with the stimulation ratio r at a given angle θ of the electrodes. All values for the average strength $\overline{w}_{AS}$ are significantly higher than 0.5 for $r\geqslant 0.6$. The system of agglomerating particles in all cases exhibits Hebbian learning.

The error bars reveal the maximum and minimum values of $\overline{w}_{AS}$ for the five sequences performed for each r. The deviations of the strengths $\overline{w}_{AS}$ from the mean value are significantly smaller for $r=0.75$ ($T_A=15$ s, $T_B=5$ s) than the deviations for both higher and lower values of r. For

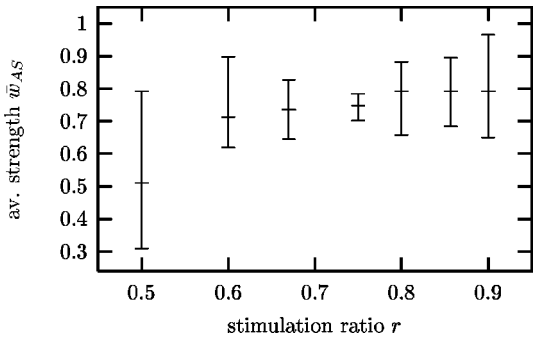

FIG. 5. Average strength $\overline{w}_{AS}$ as a function of the stimulation ratio r at $C_p=2.5/\text{cm}^2$, $\theta=60°$. The mean strength of connection A-S increases with r. The deviations of $\overline{w}_{AS}$ from the mean value are smaller in the vicinity of $r=0.75$, where $T_A=15$ s and $T_B=5$ s.

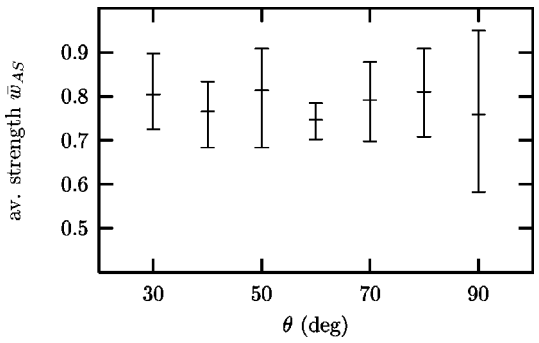

FIG. 6. The average strength $\bar{w}_{AS}$ of the connection *A*-*S* versus angle θ at $d=3$ cm, $r=0.75$, $C_p=2.5/\mathrm{cm}^2$. In the vicinity of $\theta=60°$ the deviations of $\bar{w}_{AS}$ from the mean value are significantly smaller than for other angles.

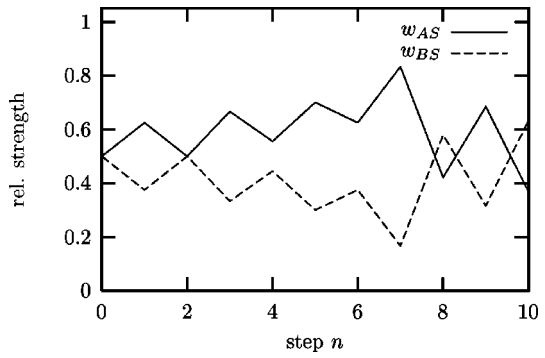

FIG. 7. Relative strengths w_{AS} and w_{BS} after each step at $d=3$ cm, $\theta=30°$, $r=0.67$, $C_p=2.5/\mathrm{cm}^2$. The electrodes *A* and *B* are close to each other; hence the wire that takes several voltages steps to form at electrode *S* subsequently oscillates between *A* and *B*.

the figure's lower *r* values, both connections exist for nearly the same time and compete for the particles. If one connection is slightly stronger during the first steps in the voltage series, the currents I_{ij} in Eq. (1) are higher and the resulting forces on the particles in the vicinity of this connection are larger. Therefore fluctuations in the initial distribution have a larger impact on the resulting strength. For $r=0.5$ both connections are used for exactly the same time and $N_B>N_A$ is as likely as $N_A>N_B$. The average strength $\bar{w}_{AS}$ varies considerably although the mean value is 0.5 in Fig 5.

Higher *r* values yield a nearly complete wire between *A* and *S*. After the voltage switches to *B*, not only single particles, but the entire *A*-*S* wire, particularly its end closest to *A*, moves toward the *B*-*S* axis. A long wire can be more mobile than either a short one or many isolated particles. In particular, an efficient way to obtain a high average strength $\bar{w}_{AS}$ with only small deviations from the mean value is to avoid a stimulation ratio for which $r\approx 1$.

A comparison of the average strengths $\bar{w}_{AS}$ for which θ is the lone independent variable shows (see Fig. 6) a similar variation in error bar length. For large angles both connections can develop rather independently and the $\bar{w}_{AS}$ can have large deviations from the mean value of $\bar{w}_{AS}$, since small variations in the initial distribution of the spheres determine the subsequent strength of each connection. At small angles θ the connecting wire tends to oscillate between the two electrodes.

The percent of change, which this oscillation produces in the connection strength, is significant for both low and, especially, high values of *r*. Figure 7 shows the evolution of w_{AS} and w_{BS} for $r=0.67$ and $\theta=30°$. Because the competing electrodes *A* and *B* are closer to each other than to electrode *S*, the effective counterelectrode in this case is the end of the oscillating wire rather than *S*. The particles in the wire originating from electrode *S* in Fig. 8 contribute to w_{BS} in step 8 and step 10 [Fig. 8(a) and Fig. 8(c)], but the same particles contribute to w_{AS} in step 9 [Fig. 8(b)]. The result is a smaller average strength $\bar{w}_{AS}$.

Figure 7 is for $\theta=30°$ and $r=0.67$. For $\theta=30°$ and $r=0.75$, the wire oscillates less, as depicted in Fig. 6.

In the vicinity of $\theta=60°$ the deviations of $\bar{w}_{AS}$ from the mean value of $\bar{w}_{AS}$ are small compared to the deviations for either higher or lower θ. At $\theta=60°$, *A* and *B* are not closer to each other than to *S*, as they are for $\theta=30°$, and the oscillations described above are hence less.

Also, if the voltage is applied to *A*-*S*, at $\theta=60°$ the forces on the particles in the vicinity of the axis *B*-*S* are higher than for larger angles. The changes induced in the wires and surrounding free particles along the *B*-*S* axis when the voltage is applied to *A*-*S*, or along the *A*-*S* axis when the voltage is applied to *B*-*S*, are greater than for $\theta>60°$. In other words, at $\theta=60°$ the cyclical application of these larger forces minimizes the effects of random initial conditions more effectively than at higher angles.

In conclusion we have shown that Hebbian learning is possible in a system of agglomerating particles in an electric field. Sequential changes in the boundary conditions can be interpreted as stimulation or training of the system, because information about these changes is still present in the system after the electric field is removed. The effect of training is found to be most stable near $r=0.75$ and $\theta=60°$. For these values the average strength $\bar{w}_{AS}$ of the resulting connection is very reproducible. For higher and lower values of θ or *r*, the resulting strengths of the connections vary more widely.

The process of thermal hopping of metal atoms on a semiconductor surface has similar dynamics when an electric field is applied. The hopping probability is enhanced in the direction along the electric field. Numerical calculations show the formation of nanowires for Au atoms on a Si surface between two electrodes at room temperature [13]. The dynamics of the Au atoms between three or more electrodes with changing boundary conditions should yield structures similar to those investigated in this paper. Therefore, the

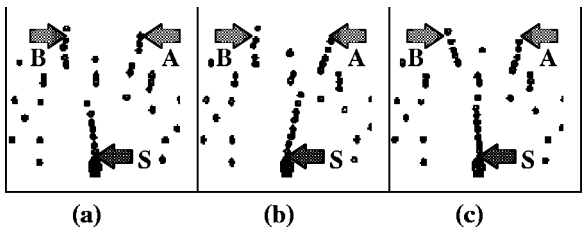

FIG. 8. (a) Step 8, (b) step 9, and (c) step 10 from the dynamics shown in Fig. 7 at $d=3$ cm, $\theta=30°$, $r=0.67$, $C_p=2.5/\mathrm{cm}^2$. The wire originating from electrode *S* switches from *B* to *A* and back and contributes to w_{AS} and w_{BS} alternately.

implementation of a neuronal network on a Si surface would be possible at a suitable range of parameters.

The main advantage of this approach for the implementation of a Hopfield network on a semiconductor chip as proposed in [14,15] would be a relatively easy method to produce and change the desired high-resistance connections, which are difficult to produce in standard complementary metal oxide semiconductor (CMOS) technology [16,17]. The network could also be retrained during the operation of such a device. Retraining is currently possible in networks where active electronic devices represent the weights [18]. This implementation comes with the drawback of losing information when the device is turned off. In contrast to that, a device based on self-assembling nanowires is nonvolatile in the sense that information once stored in the weights of the connections is still present, even if the device is turned off.

This work was supported by the U.S. ONR under Grant No. N00014-96-1-0335 and DARPA under Grant No. N00014-95-1000.

[1] D. O. Hebb, *The Organization of Behavior* (Wiley, New York, 1949), Chap. 4.

[2] J. J. Hopfield, Proc. Natl. Acad. Sci. USA **79**, 2554 (1982); reprinted in *Neurocomputing: Foundations of Research*, edited by J. A. Anderson and E. Rosenfeld (MIT Press, Cambridge, 1988), Chap. 27.

[3] J. Hertz, A. Krugh, and R. G. Palmer, *Introduction to the Theory of Neuronal Computing* (Addison-Wesley, Redwood City, CA, 1991), Chaps. 2 and 8.

[4] J. S. Langer, Rev. Mod. Phys. **52**, 1 (1980).

[5] T. A. Witten and L. M. Sander, Phys. Rev. Lett. **47**, 1400 (1981).

[6] P. Meakin, Phys. Rev. A **27**, 604 (1983).

[7] L. M. Sander, P. Ramanlal, and E. Ben-Jacob, Phys. Rev. A **32**, 3160 (1985).

[8] B. Merté, P. Gaitzsch, M. Fritzenwanger, W. Kropf, A. Hübler, and E. Lüscher, Helv. Phys. Acta **61**, 76 (1988).

[9] B. Merté, G. Handwich, B. Binias, P. Deisz, A. Hübler, and E. Lüscher, Helv. Phys. Acta **62**, 294 (1989).

[10] M. Dueweke, Ph.D. thesis, University of Illinois at Urbana-Champaign, 1997 (unpublished).

[11] W. Wen and K. Lu, Phys. Rev. E **55**, R2100 (1997).

[12] M. Dueweke, U. Dierker, and A. Hübler, Phys. Rev. E **54**, 496 (1996).

[13] S. Kümmel and A. Hübler, *Self-Assembling Electrical Connections on a Nanoscale*, Beckman Institute, University of Illinois Technical Report CCSR-95-6, 1995 (unpublished).

[14] J. J. Hopfield, Proc. Natl. Acad. Sci. USA **81**, 3088 (1984); reprinted in *Neurocomputing: Foundations of Research* (Ref. [2]), Chap. 35.

[15] J. J. Hopfield and D. W. Tank, Science **233**, 625 (1986).

[16] H. P. Graf, L. D. Jackel, R. E. Howard, B. Straughn, J. S. Denker, W. Hubbard, D. M. Tennant, and D. Schwartz, in *Neuronal Networks for Computing*, edited by J. S. Denker (AIP, New York, 1986).

[17] M. A. Sivilotti, M. R. Emerling, and C. A. Mead, in *Neuronal Networks for Computing* (Ref. [16]).

[18] M. A. Sivilotti, M. A. Mahowald, and C. A. Mead, in *Advanced Research in VLSI: Proceedings of the 1987 Stanford Conference*, edited by P. Losleben (MIT Press, Cambridge, 1987).